Ambiguity Resolution in Amplitude Comparison-Based Monopulse Direction Finding Antenna Systems

Noman Ahmad, Haq Nawaz, Nosherwan Shoaib, Qammer H. Abbasi and Symeon Nikolaou

***Abstract*—In this letter, the use of orthogonal switched-beams at θ = ±20º is proposed to improve the robustness against angle-of-arrival (AoA) ambiguities in amplitude comparison monopulse systems compared to the conventional use of only sum (Σ) and difference (Δ) patterns. As monotonic behavior of monopulse function inside the given field-of-view causes angular ambiguity so such false detection can be mitigated while analyzing the echo signal through additional switched beams. Theoretical and experimental results using a corporate-fed 1×2 patch array antenna integrated with 3 dB / 180º and 3 dB / 90º hybrid couplers, which synthesizes a sum, difference patterns and two orthogonal switched beams (θ = ±20º) at 3 GHz, endorse this improvement. The proposed antenna system can also find applications in sequential lobing based direction finding systems.**

***Index Terms*—direction-of-arrival, mono-pulse, orthogonal switched beams, sequential-lobing.**

I. Introduction

Monopulse antenna systems have attracted a lot of attention in radar, military and other wireless communication applications where determining the direction-of-arrival (DoA) [1-2] is required. They are well known due to their high speed, high accuracy, and target estimation through a single pulse. In amplitude comparison monopulse technique, due to absence of phase information, the echo signal inside the field-of-view (FoV) region can create angular ambiguities, which causes false angle-of-arrival (AoA) estimation. Two mechanisms to mitigate such angular ambiguities in conventional monopulse antenna systems are reported in [3-4]. In [3], the RF-multiplier was used to determine the sign associated with the AoA. Such phase comparators increase the cost of the system at higher frequencies. Likewise, a beam-broadening approach is described in [4] to remove the angular ambiguity in AoA. In [5-7], mechanically rotated antennas have also been employed to determine the AoA without angular ambiguity.

In this method, the associated monopulse function (Δ/Σ) is obtained through the signals received from the two antennas. Although, the angular ambiguity has been resolved using mechanically rotated two antennas, however this non-planar geometry can only be used in passive direction finding (DF) antenna system due to absence of sum (Σ) pattern. Moreover, this method also reduces the resultant FoV of monopulse function. As, these switched beams have been synthesized mechanically, the same can be realized with planar antenna by employing the 3 dB / 90º hybrid coupler as presented in this work.

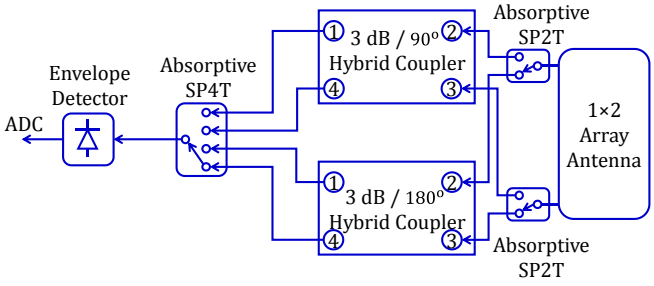

Fig. 1. Block diagram of the proposed DF antenna system.

In this letter, a new mechanism is proposed for the improvement of amplitude comparison robustness against false detection while deploying a simple planar-antenna system. It is based upon the use of two additional orthogonal switched beams (θ = ±20º) along with sum and difference patterns. The orthogonality in antenna beams reduces the interferences in the directions where other switched beams have their relative maxima. Thus, the two orthogonal switched beams have been employed to mitigate such interferences.

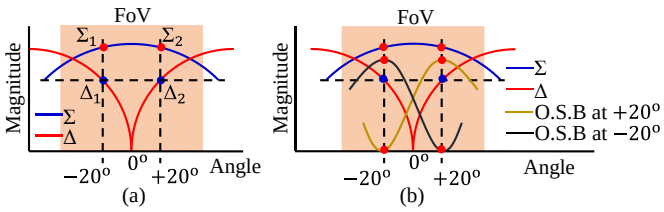

Fig. 2. (a). Conventional sum (Σ) and difference (Δ) patterns for monopulse synthesis ; (b). Proposed orthogonal switched beams with Σ and Δ patterns.

Section II discusses the theoretical back ground of the presented DF antenna system to address the angular

Manuscript received Month DD, YYYY; revised Month DD, YYYY; accepted Month DD, YYYY. Date of publication Month DD, YYYY; date of current version Month DD, YYYY. (*Corresponding author: Nosherwan Shoaib.*)

Noman Ahmad and Nosherwan Shoaib are with the School of Electrical Engineering and Computer Science (SEECS), National University of Sciences and Technology (NUST), Islamabad, 44000, Pakistan. (Email: nahmad.msee21seecs@seecs.edu.pk; nosherwan.shoaib@seecs.edu.pk)

Haq Nawaz is with Electrical Engineering, University of Engineering and Technology (UET), Lahore, 54890 Pakistan. (Email: haq.nawaz@uet.edu.pk)

Qammer H. Abbasi is with James Watt School of Engineering, University of Glasgow, Glasgow, UK (Email: Qammer.Abbasi@glasgow.ac.uk)

Symeon Nikolaou is with Frederick Research Center and Electrical Engineering, Frederick University, 1036, Nicosia, Cyprus (Email: s.nikolaou@frederick.ac.cy)

Digital Object Identifier XXXXXXXX

ambiguities which may occur in conventional monopulse antennas. The prototype of the proposed antenna system and the experimental results are described in section III.

II. Operation Mechanism

The block diagram of the proposed DF antenna concept is shown in Fig. 1. The SP2T switches are utilized to interconnect the intended hybrid couplers with the antenna ports independently. The SP4T switch is incorporated in the circuit to interconnect the output ports of the hybrid couplers with a single envelope detector for a cost effective solution. The hybrid couplers are used as feeding network to synthesize the time-shared Σ, Δ patterns and orthogonal switched beams. In conventional monopulse systems, for instance at θ = ± 20°, the echo signals captured through Σ and Δ channels create equal amplitudes i.e., $\Sigma_1=\Sigma_2$ and $\Delta_1=\Delta_2$ which causes the ambiguity in AoA estimation as shown in Fig. 2(a). To resolve such ambiguity, two switched beams are introduced to distinguish the sign (+or-) associated with AoA as indicated in Fig. 2(b). In that case, a unique amplitude is captured from these switched beams to determine the accurate AoA.

A. Amplitude comparison monopulse DF

Based on the array factor theory, two isotropic point sources, spatially displaced by 0.75λ apart when excited with equal amplitude and phase difference of 0° /180°, the Σ and Δ patterns are synthesized respectively [8-9].

$$f(\theta) = \Sigma = \cos(\beta d/2 \times (\sin(\theta)) \quad (1)$$

$$f(\theta) = \Delta = \cos(\beta d/2 \times (\sin(\theta)) \quad (2)$$

$$\Delta/\Sigma = \tan(\beta d/2 \times (\sin(\theta)) \Rightarrow \theta = sin^{-1}(\lambda/\pi d \times tan^{-1}(\Delta/\Sigma)) \quad (3)$$

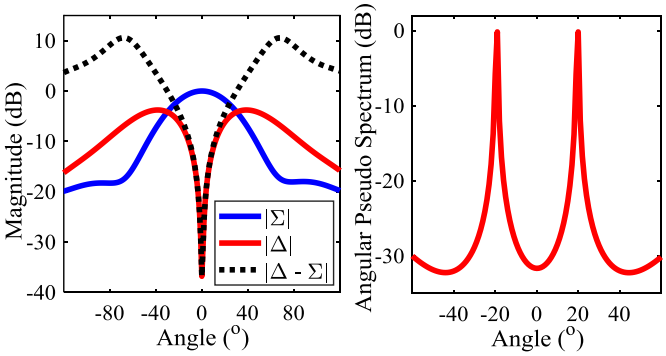

Fig. 3. Left Side: Simulated normalized sum (Σ) and difference (Δ) radiation patterns and the equivalent characterized monopulse function (Δ/Σ) ; Right Side: Simulated Angular Pseudo Spectrum (APS) for the incident signal at θ = 20°

The equation (3) indicates that the AoA can be estimated by taking the ratio of Σ and Δ signals. The simulated Σ and Δ patterns and the calculated characterized mono-pulse function (Δ/Σ) are plotted in Fig. 3. In Δ-pattern, the null depth is observed to be less than -33 dB. The obtained FoV of 60° covers the sector spanning over +30° to -30°. The mono-pulse function is monotonic as it does not have unique value for a given AoA (θ) in the obtained FoV. For instance, for a given FoV, the mono-pulse function gives value of 0.1113 (linear) for θ = ±20°. So, a signal approaching from elevation angle (θ) of 20° can be interpreted as a signal coming from θ = -20° thus leading to false AoA estimation. This ambiguity emerges only when only the amplitude of the received signals is considered for the DF estimation. In Fig. 3, this is also illustrated through angular pseudo spectrum (APS) obtained when the mono-pulse value of the received signals is compared with the characterized monopulse function [4].

$$\text{APS}(\theta) = 20log_{10}(\Sigma/\Delta(\theta) - \Sigma/\Delta_{measured}) \quad (4)$$

In Fig. 3, the simulated APS is plotted for an incident signal at θ =20°. In that case, the magnitude of the power received through the Σ and Δ channels lead to a mono-pulse function value of 0.1113 (linear), it creates a peak in the APS at the actual AoA = 20°. However, there is also another peak at θ = -20° in the same FoV. This ambiguity is caused by the monotonic behavior of the mono-pulse function. Consequently, due to lack of phase information in amplitude-comparison monopulse systems, the sign associated with the AoA cannot be determined. Based on antenna array theory, if a signal coming from elevation angle (θ) impinges upon the array elements with inter-element spacing of 'd', it experiences a relative phase difference (α) among the elements [9].

$$\alpha = \beta \times d \times \sin(\theta); \Rightarrow \theta = \sin^{-1}(\alpha/1.5\pi) \quad (5)$$

The graphical representation of equation (5) is given in Fig. 5, that shows the relationship between the AoA and the corresponding 'α' among the array elements. For AoA > 0°, the 'α' < -0° likewise the α' > -0° for AoA < -0°.

To compute the relative phase difference between the incident signals, phase-based power summation property of the 3 dB / 90° hybrid coupler is exploited. The phasor form representation of associated outputs in terms of input currents for 3 dB / 90° hybrid coupler can be expressed as follows:

$$\boldsymbol{O_1} = (-0.707 \times (j\boldsymbol{I_2} + \boldsymbol{I_3})); \boldsymbol{O_2} = (-0.707 \times (j\boldsymbol{I_1} + \boldsymbol{I_4})) \quad (6)$$

$$\boldsymbol{O_3} = (-0.707 \times (\boldsymbol{I_1} + j\boldsymbol{I_4})); \boldsymbol{O_4} = (-0.707 \times (\boldsymbol{I_2} + j\boldsymbol{I_3})) \quad (7)$$

It is evident from (6) and (7) that the amplitudes of the outputs' signals vary based upon the phase of the input signals. For instance, $I_1 \angle 0°, I_4 \angle 90°$ and $\mathbf{I_2} = \mathbf{I_3} = 0$, then $\mathbf{O_1}$= $\mathbf{O_4}$= 0 and the resulting outputs $\mathbf{O_2}$, $\mathbf{O_3}$ would be 0 and $-\sqrt{2}I_1$ respectively. The basic vector notation of input signal and the resultant output signal for 3 dB / 90° hybrid coupler is also mentioned in Fig. 4. When signal 'I_1' at port-1 lags the signal 'I_4' at port-4 by a phase of 90°, both $I_1$and I_4 add constructively at port-2 and destructively at port-3, as shown in Fig. 4 (a). Likewise, I_1 and I_4 add destructively at port-2 but constructively at port-3, when signal 'I_1' at port-1 leads the signal 'I_4' at port-4 by a phase of 90°, as mentioned in Fig. 4 (b). For any other phase difference at port-1 and port-4, the output would be the vector sum of the that input signals. Next, to analyze the phase-based power summation property 90°

hybrid coupler, the relative phase difference between the input signals has been varied from -180^o to 180^o and the resultant magnitude of the output signal has been observed. The simulated magnitude of the output signals i.e., V_2 and V_3 of 3 dB / 90° hybrid coupler versus phase variation between applied signals i.e., V_1 and V_4 is plotted in Fig. 5.

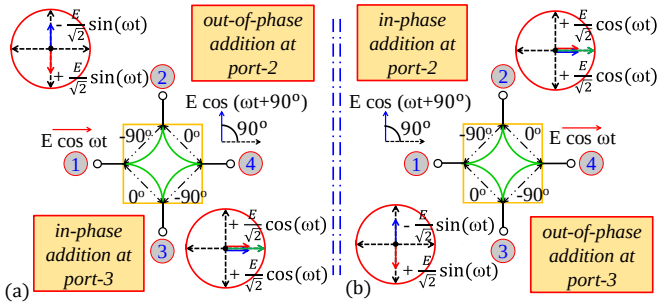

Fig. 4. Basic vector notation of the input and output signals for 3 dB / 90° hybrid coupler, (a) port-1 lags port-4 by a phase of 90° and (b) port-1 leads port-4 by a phase of 90°.

It is evident that $V_2 > V_3$ for $0^o<\alpha<90^o$ (or $0^o<\theta< 20^o$) and $V_2 < V_3$ for $-90^o<\alpha<0^o$ (or $-20^o<\theta<0^o$). The maxima of V_2 and V_3 exist at $\alpha = 90^o$ ($\theta = 20^o$) and $\alpha = -90^o$ ($\theta = -20^o$) respectively. Likewise, the minima of V_2 and V_3 exist at $\alpha = -90^o$ ($\theta = -20^o$) and $\alpha = 90^o$ ($\theta = 20^o$) respectively.

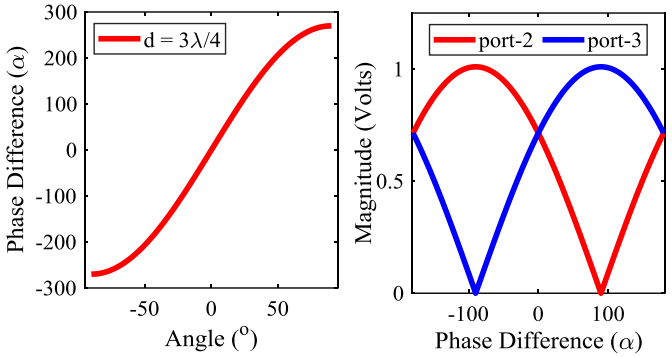

Fig. 5. Left Side: Simulated relative phase diffrence (α) with respect to the angle of arrival (θ) for inter-element spacing equal to 0.75λ ; Right-Side: Simluated amplitude of the output voltage signals at port-2 and port-3 of the quadrature coupler versus relative phase variations (α) between input ports.

Thus the interconnection of 90° hybrid coupler with 1×2 array antenna generates two orthogonal switched beams at the elevation angle (θ) of 20^o and -20^o in the *xoz-plane*. It can also be observed that the maximum gain and the null of both orthogonal switched beams are equivalent to voltage response of the 90° hybrid coupler in terms of its maxima and minima. Consequently, the sign (+ or -) associated with AoA can be measured through relative amplitudes of the 90° coupler.

The timing diagram showing the compatibility of transmitted pulse with four switched beams in reception mode is shown in Fig. 6. A pulse with duty cycle for instance 30% is transmitted through sum-pattern and corresponding echo signal is captured in listening time through four switched beams as shown in Fig. 6. On rising edge of echo signal i.e., $(T=\tau_o+\tau_1)+\tau_3$ *sec*; the antenna system will capture the echo signal for time 'τ_2' *sec* through the sum-pattern. Next, at '$T+\tau_2+2\tau_3$' *sec*; the antenna system will switch to Δ-pattern and it will receive the echo signal again for time 'τ_2' *sec*. Similarly, it will receive the echo signal through ±20° switched beams at '$T+2\tau_2+3\tau_3$' *sec* and '$T+3\tau_2+4\tau_3$' *sec* respectively for the time 'τ_2' *sec*. The 'τ_2' incorporates the rise and fall time of SP2T and SP4T switches. With reference to Fig. 6, the signal captured through pulse-1 and pulse-2 will be used for the estimation of AoA, whereas the magnitude of pulse-3 and pulse-4 would be compared to determine the sign (±) associated with AoA.

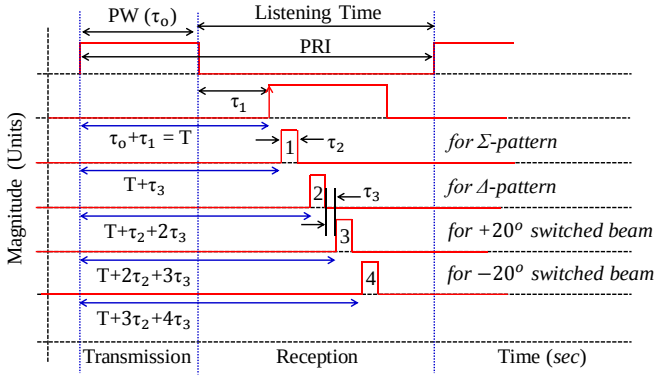

Fig. 6. Timing diagram showing the compatibility of transmitted pulse with the four switched beams in reception mode; τ_1: round trip time ; PRI : pulse-repetition interval ; τ_2: time slot assigned to receive the echo signal through respective switched beams (20% of the pulse width (τ_o)) ; τ_3: it incorporates the rise and fall time of SP2T and SP4T switches (5% of the pulse width (τ_o)).

B. Amplitude-comparison based sequential-lobing DF

In sequential lobing, time-shared multiple switched beams are synthesized to locate the object's position by comparing the amplitude of the echo signal through each switched beam. The "DF Slope (m)" is the one of the important figure-of-merit, for instance, DF slope of 0.8 dB/deg means that every 1° of angle deviation induces an amplitude variation of 0.8 dB, however, it also reveal that that the amplitude measurement error of 1 dB causes the error (1 dB)/(0.8 dB/deg) = 1.25° in measured AoA. Next, in practical scenario, the direction finding accuracy is defined over a fixed SNR. The DF accuracy will be degraded when noise level increases.

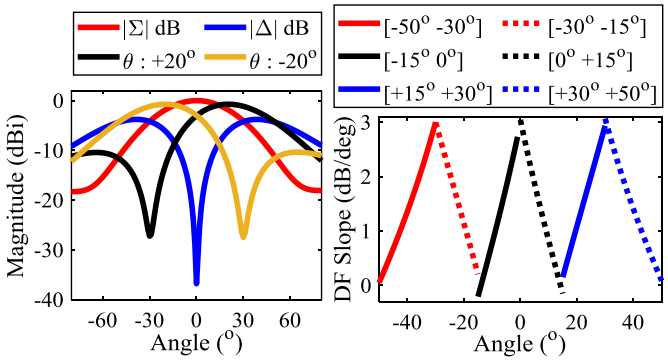

Fig. 7. Left Side: Simulated time-shared beams for the sequential lobing based DF. ; Right Side: Simulated DF slopes (dB/deg) versus the angle-of-arrivals (AoA).

The four switched beams will be comprised of sum, difference and two switched patterns at elevation angle (θ) of 20°, and -20° respectively for 'α' set to 0°, 180°, 90° and -90°. The required value of 'α' is realized through the 90° and 180° hybrid couplers. The simulated radiation patterns of the time-shared switched beams are plotted in Fig. 7. The simulated DF slopes for different ranges of the AoA are also plotted in Fig. 7. Using the radiation patterns, the DF slopes are calculated by subdividing the entire FoV into sub-ranges based upon the intersection of two consecutive radiation patterns in magnitude ≥ -3 dB. For given subrange, the pattern with greater magnitude is subtracted from pattern with lesser magnitude to obtain the DF slopes for that subrange of AoA. The minimum DF slope is reported to be 0.2 dB/deg for 0° to +15° sector. The simulated DF slopes are linear, so the AoA can be determined without any ambiguity.

III. IMPLEMENTATION AND EXPERIMENTAL RESULTS

To validate the proposed DF antenna system, the two-port vertically polarized, 1×2 edge-fed square shaped patch array antenna, along with the 180° ring hybrid coupler and the 3 dB /90° hybrid coupler are fabricated using low-cost FR-4 substrate (ε_r= 4.4, tanδ = 0.02 and thickness =1.6 mm), as presented in Fig. 8. The 90° and 180° hybrid couplers are connected to the input ports of the 1×2 array antenna using amplitude and phase matched RF coaxial cables as shown in Fig. 8 [10].

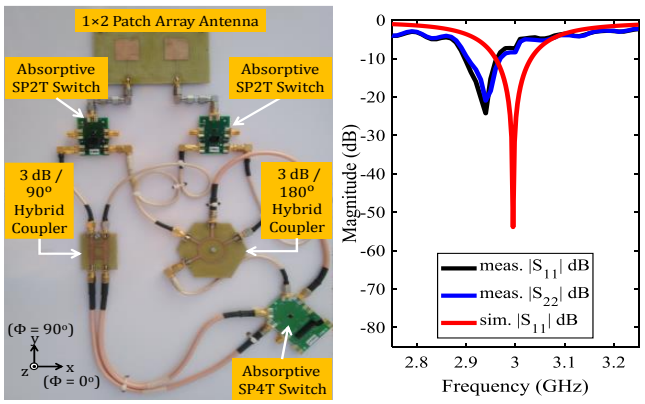

Fig. 8. Left Side: Photograph of proposed DF antenna system ; Right Side: Measured reflection coeffiecients for the prototype of 1 × 2 array antenna.

For the given length, the maximum insertion loss of coaxial cables is recorded to be 0.643 dB whereas the hybrid coupler provides the 3 dB coupling from the input to output ports at f_o = 2.94 GHz. The simulated and measured reflection coefficients for the prototype of the array antenna are given in Fig. 8. The results indicate that both ports are well matched with -10 dB impedance bandwidth of 60 MHz ranging from 2.90 to 2.96 GHz. The frequency shifts between the simulated and measured results can be caused by the various factors including variations in the dielectric constant of substrate, fabrication errors etc. At f_o = 2.94 GHz, the simulated and measured monopulse function (Δ/Σ) is in well agreement for a FoV [-30° +30°] as shown in Fig. 9. To validate the system performance, the measured DoA estimations along with angle estimation error i.e., root-mean-square-error (RMSE) are also presented in Fig. 9. The measured AoA has been determined using (3) with measured monopulse function (Δ/Σ). The results show that, maximum RMSE is recorded to be less than 5° for given FoV of 60° ranges from -30° to +30° except at -20° where RMSE is noted to be 8.9°. It can also be observed that due to monotonic behavior of monopulse function, the measured AoA is same for both negative and positive angle-of-arrivals. This angular ambiguity would be resolved while comparing the amplitude of received signal from the additional switched beams as described in Section II.A. The radiation patterns of the presented array antenna have been characterized in the 360° span (θ = 180° to θ = -180°) for both φ = 0° and φ = 90° in anechoic chamber.

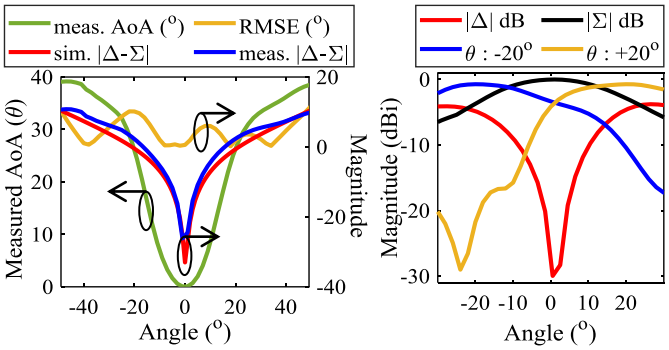

Fig. 9. Left Side: Simulated and measured relationship between the monopulse function (Δ/Σ) and AoA (θ) at 2.94 GHz, measured AoA and RMSE ; Right Side: Measured normalized gain plots of the four switched beams at 2.94 GHz in the *xoz-plane*.

Due to antenna's geometry, the main beam will be switched in *xoz-plane*. For the sake of brevity, the measured normalized gain plots at 2.94 GHz in the *xoz-plane* are plotted in Fig. 9. The maximum measured peak gain for the sum-pattern and difference pattern is recorded to be respectively 5.97 dBi and 3.97 dBi with radiation efficiency of 55%. Likewise, the magnitude of two switched beams and null depth of difference pattern is recorded to be 5.1 dBi and -25 dB respectively. The gain difference between simulated and measured patterns is because of surface roughness of copper, loss tangent (tanδ) of substrate and fabrication errors. Consequently, the proposed antenna system can be employed to compute the DoA while resolving the angular ambiguity in the FOV using additional switched beams.

IV. CONCLUSION

In this work, a planar antenna system is presented for amplitude comparison-based DF. To validate the concept, the antenna system is designed for 3 GHz, however this concept is valid for higher frequencies i.e., > 3 GHz. The DF estimation is realized through the mono-pulse and sequential-lobing techniques. In amplitude monopulse antenna systems, to address the angular ambiguity in sign (+or-) associated with AoA, phase-based power summation property of 90° hybrid coupler and the corresponding switched-beams is utilized.

V. Acknowledgement

This research was co-funded by the European Regional Development Fund and the Republic of Cyprus via the Research and Innovation Foundation through the EXCELLENCE/ 0421/0495 – SMURFS project.

References

[1] Sherman. S.M., Burton. D.K, "*Monopulse Principles and Techniques*", 2nd ed, Artech House, Norwood, MA, USA, 2011.

[2] J. Xie, X. Feng, Y. Yuan, and S. Li, "Application of monopulse techniques in angle-measuring of single-beam mechanical scanning radar," *Proc. 3rd Int. Congr. Image Signal Process*., pp. 2971–2974, 2010.

[3] Rashid, Rimi et al. "A Planar Extended Monopulse DoA Estimation Antenna Integrating an RF Multiplier." *Progress in Electromagnetics Research C* 81, pp. 53-62, 2018.

[4] M. Poveda-García and J. L. Gómez-Tornero, "Ambiguity Resolution in Amplitude-Monopulse Systems Using Broad-Beam Patterns," *IEEE Antennas and Wireless Propagation Letters*, vol. 20, no. 4, pp. 503-507, April 2021, doi: 10.1109/LAWP.2021.3055275.

[5] Y. Álvarez-López, M. E. Cos-Gómez, and F. Las-Heras-Andrés, "A received signal strength RFID-based indoor location system,", Sensors and Actuators A: Physical, vol. 255, pp. 118–133, 2017, doi.org/10.1016/j.sna.2017.01.007

[6] M. Poveda-García *et al*., "Amplitude-Monopulse Radar Lab Using WiFi Cards," *2018 48th European Microwave Conference (EuMC)*, Madrid, Spain, 2018, pp. 464-467, doi: 10.23919/EuMC.2018.8541674.

[7] J. A. López-Pastor, P. Arques-Lara, J. J. Franco-Peñaranda, A. J. García-Sánchez and J. L. Gómez-Tornero, "Wi-Fi RTT-Based Active Monopulse RADAR for Single Access Point Localization," *IEEE Access*, vol. 9, pp. 34755-34766, 2021.

[8] C.A. Balanis,"Antenna Theory Analysis and Design," 4th edition, Wiley& Sons, New York, 2016.

[9] W.L. Stutzman and G.A. Thiele, "Antenna Theory and Design,"3rd ed, Wiley & Sons, New York, 2012.

[10] N. Shoaib, "Vector Network Analyzer (VNA) Measurements and Uncertainty Assessment," Springer, vol. 1; pp. 1-82, 2017. Available Online at: https://doi.org/10.1007/978-3-319-44772-8.